

### 3.3.3.4 Experimental determination of absolute emissions from concentration ratios by means of tracer studies

M. Möllmann-Coers, D. Klemp, K. Mannschreck

#### Introduction

In the frame of the joint research project EVA (Slemr et al. 2002b) which is focused on the evaluation of an emission model, the absolute CO emission rates of the city of Augsburg were determined by means of the source-tracer-ratio (STR) method. Applying this method several atmospheric tracer experiments were performed within two field campaigns in March and October 1998. Sulphur hexafluoride (SF<sub>6</sub>) was used as tracer which was released in Augsburg to mark the city plume. The emission rates of CO are then calculated by means of the known emission rates of SF<sub>6</sub> and the measured SF<sub>6</sub> and CO mixing ratios downwind of Augsburg. From correlation analyses between CO and other substances (NO<sub>x</sub> and NMHCs) in the plume absolute emission rates of these species were also determined.

#### Experimental

##### Principle of the source-tracer-ratio (STR) method

Tracers are widely used to study advection and dispersion processes (Pasquill 1974). For this purpose, suitable species have to be chemically inert and not toxic and have not to be present in the normal environment. SF<sub>6</sub> fulfils these requirements to a large degree and it can be measured in the low ppt range by electron capture detector technique (ECD). A brief overview of the experimental technique is given by Zeuner and Möllmann-Coers (1994).

When using the STR method the unknown emissions of a species (in our case CO) are marked by a tracer (in our case SF<sub>6</sub>) released with a known emission rate. Providing a comparable distribution of CO and SF<sub>6</sub> sources and assuming identical atmospheric transport and dispersion of SF<sub>6</sub> and CO, the emission rate of CO can be calculated from the concentration ratio and the known SF<sub>6</sub> emission rate according to equation (3.8):

$$\dot{q}_{CO} = \frac{c_{CO}}{c_{SF_6}} \dot{q}_{SF_6} \quad (3.8)$$

In this equation  $\dot{q}_{CO}$  is the unknown emission rate of CO,  $\dot{q}_{SF_6}$  is the known emission rate of SF<sub>6</sub>, and  $c_{CO}$  and  $c_{SF_6}$  are the measured concentrations of CO and SF<sub>6</sub>, respectively.

### ***Tracer release and sampling***

The experimental site and the locations of the tracer release and receptor sites are shown in Fig. 3.20. Under southwesterly wind conditions SF<sub>6</sub> is released at position 1 to 9 in the city with a known emission rate. The large number of release positions provides for a homogeneous build-up of the SF<sub>6</sub> plume comparable to that of the respective CO emission plume. Air samples were taken along the reception line downwind of Augsburg. The reception line consists of 16 individual sampling positions.

Conducting the experiments, pure SF<sub>6</sub> is released directly from gas cylinders with a constant emission rate of 1 g/s. The release height is 4m above ground.

The samplers for up to 9 sampling bags (aluminium coated plastic bags Linde Plastigas®) were designed and built by Research Centre Jülich. The air samples are taken about 1 m above ground. The time base for the individual samplers is given by a radio controlled clock and the begin and the end of the sampling period can be set individually for each sample.

### ***Gas analysis***

The SF<sub>6</sub> concentrations in the air samples were analysed using a gas chromatograph (Siemens, Sichromat 3) equipped with an ECD. The samples were analysed for CO using the fast-response resonance fluorescence method described by Gerbig et al. (1996, 1999) and Volz-Thomas and Gerbig (1998). More details of the analysis technique are given in Möllmann-Coers et al. (2002a).

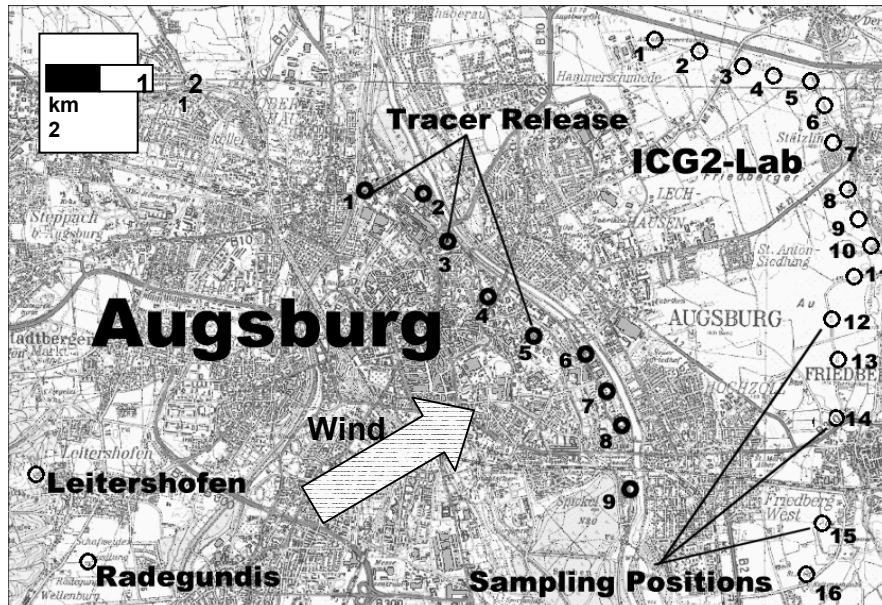


**Fig. 3.20.** Experimental site and experimental design. The downwind positions of the sampling units are shown on the right in the figure, as well as the upwind positions at Radegundis and Leitershofen on the left side. The tracer release positions are depicted in the centre of the figure. In addition, the position of the ICG II mobile laboratory is marked. Position 7 of the reception line is identical with the position of the ICG II mobile laboratory. By means of this laboratory a wide range of hydrocarbons as well as CO and NO<sub>x</sub> have been measured (Klemp et al. 2002).

### **Application of the STR method in Augsburg**

#### **Using CO as a reference trace gas**

For the application of the STR method to evaluate modelled emission inventories CO was chosen as reference substance for trace gas emissions from Augsburg. The use of CO has several advantages:

1. Apart from CO<sub>2</sub>, CO is by far the most abundant species released from anthropogenic sources.
2. CO is nearly exclusively emitted by combustion processes and especially by vehicle exhaust (Kühlwein et al. 2002a). Within the Augsburg area there are only very small CO-emitting point sources (Kühlwein et al. 2002b). Consequently the assumption of an area source for CO (as requested for the STR method) is met with good approximation. The emission rates of other mainly traffic-related species like NO<sub>x</sub> and some NMHCs (i.e. benzene, ethyne, ethene) can be calculated from their concentration ratios to NO<sub>x</sub>.

3. Within the advection time from the release to the sampling position (0.5 h), CO can be assumed to be inert.

The main disadvantage of CO is its relatively high atmospheric mean CO background, which exceeds the impact of the city emissions downwind of Augsburg.

### ***Experimental design***

The experimental design is depicted in Fig. 3.20. For the chosen conditions the city plume of Augsburg can be approximated by a line of point sources through the city for southwesterly winds. This is shown by detailed model studies (Möllmann-Coers et al. 2002a). The tracer sampling line is established about 3 km easterly of the city. The area between the city border and sampling line consists mainly of agricultural land without significant CO sources. The distance of three km is sufficient for a vertically well mixed city plume within the atmospheric mixing layer. The latter assumption is supported by the results of model studies mentioned above.

### ***The tracer experiments***

To ensure a clear source receptor relationship on the one hand and to receive a significant increase of the CO concentration within the city plume on the other hand, the conduction of tracer experiments was restricted to wind speeds between 2.5 and 7.5 m/s at 10m height. In addition, the experimental design restricts the experiments to southwesterly winds (cf. Fig. 3.20)

The tracer experiments last four hours from 11 to 15 local time. In order to get a stationary tracer plume, the tracer release started 20 minutes before the begin of sampling. Nine 20 minute samples were taken at each position of the receptor line. Four of six experiments could be analysed. Two were not analysed due to an unexpected wind shift during the experiment.

### ***Data analysis***

The evaluation of the experimental data requires the knowledge of the background CO and SF<sub>6</sub> concentration:

1. From test samples in Augsburg a mean SF<sub>6</sub> concentration of 7.2 ppt was found which is about 7% of the mean experimental tracer concentration at the reception line.
2. Due to its lifetime of more than 2 months background concentrations of CO may vary  $\pm 30$  ppb depending on the history of the air masses (Mannscheck 2000) for different experiments. Further, even in the city plume the CO background contributes to more than 70% (Klemp et al. 2002) to total CO levels. Consequently, the CO background has to be determined for each experiment individually using two additional sampling positions upwind of Augsburg.

3. The experimental results show that several samples are contaminated by local events e.g. occasional harvest traffic on the fields close to an individual sampling position. On the other hand, due to variations in the wind direction the city plume may not cover the whole reception line all the time. In any case, for this type of event the differences of the concentrations between two neighbouring positions exceed the  $1\sigma$ -range. Within a sampling interval these samples were excluded from the evaluation by a median-based filter algorithm:

$$\left| C_{Median}^{CO} - C_i^{CO} \right| \leq f C_{Median}^{CO}, \text{ with } f = 0.3^3. \quad (3.9)$$

The mean CO/SF<sub>6</sub> emission ratio is calculated by orthonormal regression analysis (York 1966) using the remaining pairs of CO and SF<sub>6</sub> mixing ratios after filtering and the respective background measurements performed in Radegundis and Leitershofen. The  $1\sigma$ -uncertainty of the slope ( $\approx 30\%$ ) is denoted as uncertainty of the calculated CO/SF<sub>6</sub> emission ratio. More details about the application of the STR method are discussed in Möllmann-Coers et al. (2002a).

### Results and discussion

Table 3.12 summarizes the absolute CO emission rates derived from the application of the STR method. Within the range of uncertainty, the results agree with correspondent results from a mass balance method (Kalthoff et al. 2002). It is shown that the experimentally determined emission rates also agree with the results of the emission model (Kühlwein et al. 2002a). The same is valid for the NO<sub>x</sub> emission rates listed in Table 3.12. These values were calculated from the CO values (Table 3.12) according Eq. (3.8) and from the NO<sub>x</sub>/CO concentration ratio determined from the measurements of the ICG II mobile laboratory (cf. Fig. 3.20). The uncertainties of NO<sub>x</sub> are calculated by quadratic additions of the individual uncertainties of the CO/SF<sub>6</sub>- and NO<sub>x</sub>/CO- correlations, respectively.

**Table 3.12.** Absolute CO and NO<sub>x</sub> emission rates together with their respective uncertainties

Date:	27.3.	10.10.	22.10.	23.10.
CO emission rate (t/h)	3.0±1.0	1.8±0.4	0.98±0.24	0.9±0.2
NO <sub>x</sub> emission rate (t/h)	0.35±0.12	0.25±0.06	0.24±0.07	0.22±0.05

The CO emission rate on 27<sup>th</sup> of March (a working day) is significantly higher than the CO emissions for working days in October. This is probably due to residence heating, not present in autumn.

<sup>3</sup> Sensitivity tests indicated that the choice of  $f$  within a wide range (0.1 to 3) primarily affects the uncertainties and has only weak influence on the calculated emission rates.

The ICG II laboratory at Stätzling was integrated in the STR reception line (cf. Fig. 3.20). Consequently, the NMHC/CO concentration ratios (Klemp et al. 2002) determined at Stätzling can be combined with the CO emission rates derived by STR method. Based on Eq. (3.8) the emissions rates of individual hydrocarbons can be calculated in the same way as the NO<sub>x</sub> emission rates. Table 3.13 shows the result for NMHCs which can be specified individually from the emission model results (Mannscheck 2000).

Several conclusions can be drawn from the comparison of the experimental and model results (cf. Table 3.13):

- Since the measured and modelled CO emission rates compare well within their uncertainties, significant differences between modelled and measured hydrocarbon emission rates have to be attributed to the differences in hydrocarbon emissions. Comparing the experimentally derived NMHC emission rates with the model results deviations up to a factor of 5 can be found for some species (i.e. ethane, propane). These deviations exceed by far the uncertainty of the STR method which is about 30%. For some other species (e.g. toluene), the agreement between both emission rates is quite good.
- The measurements suggest that the emission rates of most NMHCs are about twice as large in March than in October. But the model predicts - apart from the butenes and the C<sub>4</sub>-C<sub>5</sub> alkanes - the same emission rates in spring and autumn.
- The modelled emission rates of C<sub>4</sub> and C<sub>5</sub> alkanes are in October by 30% - 40% higher than in March. This is mostly due to its higher share of evaporation processes in October in comparison to the March campaign. This behaviour, however, was not observed in the experimental data, suggesting that the increase of evaporation-related emissions with increasing temperature is only of minor importance. Emission rates of C<sub>4</sub> and C<sub>5</sub> alkanes in October were smaller than those in March suggesting to combustion related emissions as the major source of C<sub>4</sub> and C<sub>5</sub> alkanes. This is in line with the conclusions of Mannscheck et al. (2002a) and Möllmann-Coers et al. (2002c).

**Table 3.13.** Absolute emission rates for a number of hydrocarbons calculated from their NMHC<sub>i</sub> /CO ratios together with their 1-s-standard deviations (Experiment) and the corresponding emissions calculated with the emission model (Model) (EVA-Database, 2000)

Date	27.3.		10.10.		22.10.		23.10.	
	Emission rate [kg/h] [kg/h]		Emission rate [kg/h] [kg/h]		Emission rate [kg/h] [kg/h]		Emission rate [kg/h] [kg/h]	
Species	Experiment	Model	Experiment	Model	Experiment	Model	Experiment	Model
Ethene	37.5±18.6	14.7	12.3±4.4	15.7	10.8±3.55	19.4	10.0±3.1	18.7
Ethyne	24.0±9.0	7.9	17.0±5.8	7.2	10.5±3.0	7.4	9.7±2.7	7.7
Ethane	13.9±7.3	2.8	8.8±3.3	5.7	7.1±3.3	11.3	6.6±3.0	6.2
Benzene	16.5±6.2	9.1	14.9±5.1	10.1	9.0±2.3	10.5	8.3±2.0	10.8
Propene	10.8±5.1	6	11.8±4.8	6.1	5.5±8.5	6.7	5.1±7.8	6.9
Propane	18.8±11.9	3.8	12.3±4.7	4.2	5.6±2.4	5.8	5.2±2.2	4.8
Butene	7.9±3.7	4.6	6.9±2.7	6.6	4.9±1.7	6.7	4.5±1.5	8.7
i-Butane	13.7±5.6	6.5	7.1±2.4	9.6	7.5±2.9	9	6.9±2.6	13.6
n-Butane	23.1±11.3	14.8	12.7±4.2	22.8	9.2±3.3	21.4	8.5±2.9	32.5
i-Pentane	25.2±9.9	29.5	17.9±6.1	42.8	7.8±2.1	40.3	7.3±1.9	59.3
n-Pentane	19.9±9.5	9	8.7±3.0	13	10.8±6.1	12.1	10.0±5.6	17.6
Toluene	39.0±18.3	38	27.6±9.0	30.2	26.7±7.8	35.6	24.7±6.9	34.7

### Summary and Conclusions

The STR method was successfully applied to determine the absolute CO emission rates of Augsburg. The results obtained with the STR method compare favourably with those obtained by the mass balance method (Kalthoff et al. 2002; Kühlwein et al. 2002a)

The overall accuracy of the STR method applied here is in the range of 30%-40%. Within the range of uncertainty the experimentally derived CO and NO<sub>x</sub> emission rates agree with the results of the emission model. But for some hydrocarbons the experimentally determined emission rates exceed from the modelled ones up to a factor of 5.

### **3.3.3.5 Determination of anthropogenic emission ratios in the Augsburg area by long-term concentration measurements downwind of the city**

D. Klemp, K. Mannschreck, F. Slemr

#### **Introduction**

Air quality models require temporally and spatially highly resolved emission inventories of NO<sub>x</sub>, CO and individual organic compounds as one of the most important input parameters. Since the quality of the output of the air quality models depends decisively on the quality of the input emission data (Placet et al. 2000), the latter has to be assessed.

In a joint project “EVALuation of calculated highly resolved emissions of a city” (EVA) within the German Tropospheric Research Programme (TFS), several institutions determined the emissions of the city of Augsburg by three independent techniques and compared the results with the calculated emissions (Slemr et al. 2002a). One of the techniques was the determination of the emission ratios from the concentration ratios measured at a ground receptor site downwind of the city and onboard aircraft. Special attention is devoted to the speciation of the hydrocarbon emissions. The question of representativity of emission measurements in Augsburg is also addressed.

#### **Experimental**

Augsburg is a medium-sized city (250,000 inhabitants) in Bavaria in Southern Germany. CO, C<sub>2</sub> – C<sub>10</sub>-hydrocarbons, NO and NO<sub>2</sub> at the receptor site were continuously measured throughout two 4 week long campaigns in March and in October 1998. For this purpose the mobile laboratory of Forschungszentrum Jülich was placed north-east of Augsburg in Stätzling in a distance of about 5 km from the city centre.

During intensives, grab samples were taken onboard aircraft circling around the city of Augsburg and analysed at IFU Garmisch for NMHC content. The samples were taken randomly upwind and downwind of the city at altitudes varying from about 150 m above ground up to the top of the mixing layer and a few samples were taken in the lower free troposphere.

#### **Analytical techniques**

The analytical instruments were installed in the air conditioned mobile laboratory of Forschungszentrum Jülich (Klemp et al. 2002). The inlets and meteorological instruments were mounted on a pneumatic mast 10 m above the surface. Briefly, CO was measured using a commercial infrared filter correlation absorption spectrometer (Thermo Environmental Instruments, Modell TE48). Interferences



by atmospheric water vapour were eliminated by drying the sampled air using Nafion<sup>®</sup> drier. Problems with zero drift were substantially reduced by passing ambient air through a Hopcalite<sup>®</sup> scrubber for 5 minutes every hour.

NO<sub>x</sub> and NO<sub>y</sub> were measured using chemiluminescence detectors (ECO Physics, CLD 770AL ppt) and a photolytic converter (ECO Physics PLC 760) to convert NO<sub>2</sub> to NO. Due to the fact that the conversion efficiency of the PLC in ambient air is affected by the mixing ratios of O<sub>3</sub> and NO<sub>2</sub> a photochemical box model is used to simulate the respective conditions in the PLC chamber (Pätz et al. 2000) and to correct the measured NO<sub>2</sub> raw signals.

Different to the other analytical equipment the NMHC measurement technique is based on a home-built GC-system, designed for the trace gas analysis in the lower ppt-level. C<sub>2</sub> – C<sub>10</sub> hydrocarbons were measured using a gas chromatograph (HP 5890A) with a flame ionisation detector (FID) and a specially designed sampling device (Schmitz T et al. 1997). Water from sampled air was removed by a cooling trap kept at –25 °C. NMHCs from a sample volume of 500 cm<sup>3</sup> were then preconcentrated in a liquid nitrogen cooled sample loop (20 cm long, 2 mm diameter) filled with glass beads. The flow of sampled air was kept at 50 ml/min resulting in 10 min sampling interval. When sampling is completed, the sample loop is heated up to 80 °C and the hydrocarbons are injected on the capillary column (DB-1, 90 m x 0.32 mm ID, film thickness: 3µm). After injection the column is kept isothermal at –50 °C for 5 min and then heated up to 200 °C with a rate of 5 °C/min. Subsequently the column temperature is kept at 200°C for 15 min. The complete analysis took about 80 minutes.

Individual peaks in the chromatogram were identified via injection of the pure species and the identification was confirmed using the 70 component gas mixture (Slemr 1999). The mean detection limits for measured hydrocarbons varied between 10 ppt (C<sub>3</sub>-compounds) and 3 ppt for hydrocarbons > C<sub>8</sub>. From error propagation analysis the experimental uncertainties ( $\Delta\mu_{\text{HC}_i}$ ) are calculated to account to less than 15% to the respective mixing ratios  $\mu_{\text{HC}_i}$  of HC<sub>i</sub>.

With respect to the NMHC grab samples taken onboard aircraft, air samples were drawn by two Metal Bellow pumps in series into 1 l electropolished stainless steel canisters. The canisters were then shipped to the laboratory and analysed: Briefly, 400 ml of air samples were directed through CO<sub>2</sub> and H<sub>2</sub>O scrubber (columns packed by NaOH and Mg(ClO<sub>4</sub>)<sub>2</sub>) and the C<sub>2</sub> - C<sub>10</sub> NMHCs were trapped at -25 °C on Carbotrap (Chrompack). The enriched NMHCs were then desorbed at 120 °C and cryofocussed on the initial part of the separation column at -120 °C. The NMHCs were separated on Al<sub>2</sub>O<sub>3</sub>/Na<sub>2</sub>SO<sub>4</sub>-PLOT column (50 m long, 0.53 mm diameter, 10 µm film thickness) using a temperature program (5 min at 50 °C, 8 °C/min up to 170 °C, 6 °C/min to 200 °C and hold for 45 min). Total uncertainty of the NMHC measurements as given by the reproducibility of the analyses including sampling and sample storage, and by the quoted uncertainty of the calibration gas mixture which was in total about 8% for alkanes, 12% for aromatic compounds, and 20% for alkenes.

The quality of ground based measurements and of the analyses of air samples in canisters was assessed by intercomparisons before and after each EVA

measurement campaign. The results of the intercomparisons with synthetic gas mixtures and ambient air measurements are described in detail by Kanter et al. (2002) and Volz-Thomas et al. (2002). It is shown in Volz-Thomas et al. (2002) that the agreement between the ground and canister NMHC measurements was usually better than 20%.

### ***Determination of emission ratios from concentration ratios***

The concentration of a pollutant measured at a receptor site downwind of a city results from the concentration upwind of the city (background) and from the mixed in and diluted emissions within the city area. For time periods of constant background concentrations and in the absence of chemical reactions, the concentration ratio of two co-emitted species remains constant, because both species are subjected to the same atmospheric mixing processes. During those conditions the concentration ratio at the receptor site of two co-emitting pollutants is determined solely by their emission ratio. The emission ratio of two pollutants is thus calculated as slope of an orthonormal correlation (York 1996) of synchronously measured concentration pairs over a period of constant background concentrations.

For a calculation of emission ratios,  $E(A)/E(B)$ , of a city from experimentally derived concentration ratios,  $\mu(A)/\mu(B)$ , downwind of the source several requirements have to be fulfilled:

- The chosen measurement site has to be located in the main wind direction downwind of the city.
- Contamination from sources near to the receptor site have to be negligible.
- The distance between the city and the receptor site has to be long enough for sufficient mixing.
- The transport time should be short enough to prevent significant photochemical removal.

As an appropriate measurement site we have selected a location 5 km northeast of Augsburg centre next to the small village Stätzing. Photochemical removal during transport is minimized by choosing time periods of lower photochemical activity (March and October). Local contamination can be neglected for the considered species since the area between Augsburg and Stätzing is used exclusively for agricultural purposes.

Emission ratios from NMHC and CO measurements in air samples taken onboard aircraft were calculated formally in the same way as described above as slopes of the orthonormal correlations. In contrast to the measurements on the receptor site at the ground, these correlations contain measurements upwind and downwind of the city area. Since the air samples were taken randomly along the flight track, all emissions within the area confined by the flight track are considered.

## Results and discussion

### Filter criteria for the ground-based measurements

Given by the analytical system with the lowest time resolution (GC-system, sampling interval: 10 min), all other data were averaged over 10 min intervals. The data from Stätzling were only considered when the site was downwind of the city. In order to ensure stable wind flow conditions, only data with wind speeds  $\geq 3$  m/s were used. 45 and 50 % of the data from March and October, respectively, met both the wind direction and speed criteria.

### Characteristic trace gas ratios for urban air masses

Since the contribution of the background may substantially exceed the impact of the city emissions (October campaign: Mean CO concentration: 201 ppb), it is indispensable to subtract the background concentrations<sup>4</sup>. This is achieved by considering concentration ratios and by calculating the emission ratios via correlation analyses. Table 3.14 lists the characteristic emission ratios of  $\Sigma\text{HC}/\text{NO}_x$ , the mean reactivity  $\langle k_{\text{OH}} \rangle$  and mean number of C-atoms  $\langle C \rangle$  together with their uncertainties and regression coefficients ( $R^2$ ) for the October campaign. The mean reactivity  $\langle k_{\text{OH}} \rangle$  and the mean chain length  $\langle C \rangle$  of the hydrocarbons are calculated as follows:

$$\langle \alpha_i \rangle = \frac{\sum_i \alpha_i \cdot \text{HC}_i}{\sum_i \text{HC}_i}, \text{ with } \alpha_i = k_{\text{OH}}^i \text{ and } \alpha_i = C^i. \quad (3.10)$$

The  $\text{CO}/\text{NO}_x$  emission ratios on weekends were more than twice as high as on working days. This is probably due to the absence of heavy duty vehicles on weekends, which are strong  $\text{NO}_x$  emitters (Hassel et al. 1995). The mean reactivity  $\langle k_{\text{OH}} \rangle$  and the mean number of C-atoms  $\langle C \rangle$  were significantly higher on weekdays than on weekends. It has been shown by Mannschreck et al. (2002a) that the mean NMHC reactivity on weekdays is substantially higher due to a larger contribution of alkenes and aromatics relatively to that of the alkanes.

<sup>1</sup> Mean CO-background values (October campaign: 165 ppb) were calculated using regression of CO against concurrently measured  $\text{NO}_x$  and extrapolating CO background concentrations to a  $\text{NO}_x$  concentration of 1 ppb (Mannschreck et al. 2002)

**Table 3.14.** Characteristic parameters of urban air masses, relative uncertainties ( $1\sigma$ ) and respective correlation coefficients ( $R^2$ ) for the October campaign (Augsburg, urban sector).

Characteristic parameters	Weekdays	Saturdays	Sundays
$\Sigma HC_i/NO_x$ [ppbC/ppb]	2.9±0.2 (0.71)	2.7±0.5 (0.47)	3.8±0.5 (0.67)
$\langle k_{OH} \rangle$ [ $cm^3 s^{-1} 10^{-12}$ ]	7.4±0.1 (0.96)	4.4±0.5 (0.78)	5.8±0.4 (0.87)
Number of C atoms $\langle C \rangle$	4.2±0.04 (0.99)	3.5±0.1 (0.97)	3.6±0.1 (0.98)
CO/NO <sub>x</sub> [ppb/ppb] (all data)	6.8±0.2 (0.82)	17.5±1.0 (0.67)	14.2±0.8 (0.59)

***Comparison of emission ratios derived from ground based measurements with those from measurements onboard aircraft***

The receptor site and the air-borne measurements are based on different fetches: Whereas the correlations from ground-based measurements result from averaging of time series of several weeks duration, the correlations from air-borne investigations yield spatial averages due to the circling of the aircraft around the city of Augsburg. It is thus important to compare the results obtained by these different techniques.

Fig. 3.21 shows a plot of average  $HC_i/\text{sum}(HC)$  emission ratios on working days from air-borne measurements versus mean emission ratios measured at Stätzing on working days in October 1998. Emission ratios determined by the two different techniques correlate well ( $R^2 = 0.93$ ). This result suggests that long-term receptor measurements of the emission ratios yield a stable hydrocarbon pattern, which can be treated as representative for the emissions of the whole city.

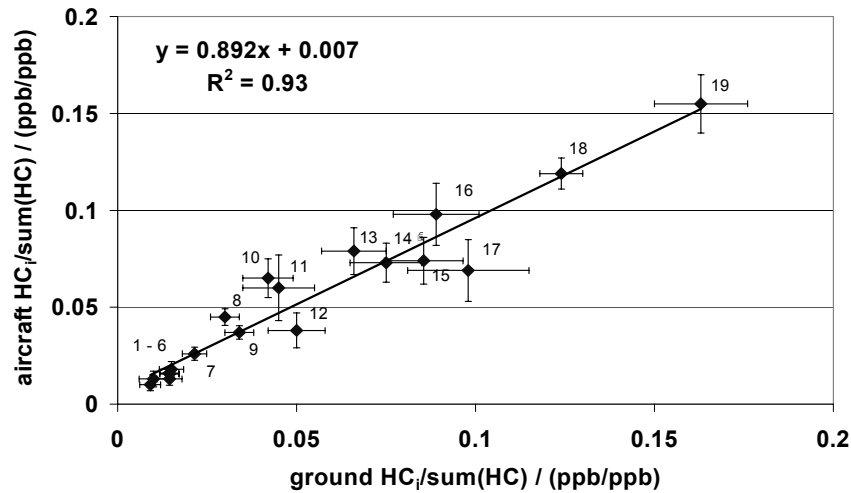


**Fig. 3.21.** HC<sub>i</sub>/sum(HC) emission ratios from aircraft measurements (mean ratios for the intensives performed on weekdays) versus HC<sub>i</sub>/sum(HC) emission ratios measured downwind of the city on the receptor site in Stätzling (mean ratios for the October campaign, weekdays). The bars represent the 1 $\sigma$  standard deviations from the regression analyses for the aircraft measurements as well as for the ground based measurements. 1: n-hexane; 2: cyclohexane; 3: heptane; 4: 2,3-methylhexane; 5: 3-methylpentane; 6: 2-dimethylbutane; 7: 2-methylpentane; 8: propene; 9: butenes; 10: i-butane; 11: n-pentane; 12: benzene; 13: n-butane; 14: propane; 15: toluene; 16: i-pentane; 17: ethane; 18: ethyne; 19: ethene. The HC<sub>i</sub>/sum(HC)-ratios are based on mixing ratios (ppb/ppb).

### **Representativity of the emission ratios measured in Augsburg**

An estimation for the representativity of the Augsburg hydrocarbon pattern for German city conditions can be obtained by comparison with an averaged NMHC emission pattern for urban conditions.

This pattern was constructed from measurements in German cities between 1982 and 1995 (Schmitz T et al. 1997; Abraham et al. 1994; Bayerisches Landesamt für Umweltschutz 1994; Bruckmann et al. 1983; Ellermann et al. 1995; Thijssse and van Oss 1997) and is given in the “Database for Volatile Organic Compounds” (Mannschreck et al. 2002b). Fig. 3.22 shows the mean hydrocarbon distribution for the Augsburg measurements and the averaged urban emission scenario taken from Mannschreck et al. (2002b). The hydrocarbon composition of both campaigns in March and October are very similar to the averaged urban emissions for German cities suggesting that the HC-composition measured in Augsburg is representative for urban scenarios in Germany.

### Summary

Long-term ground based receptor emission measurements represent a well-suited method to get a representative picture of characteristic emission ratios from a whole city.

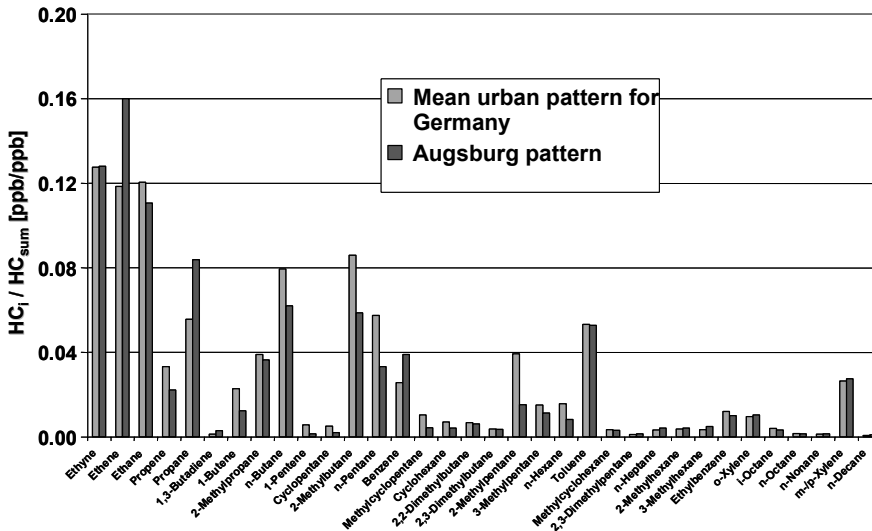


**Fig. 3.22.** Results of ground-based measurements performed during EVA (October and March) and a average HC-composition for German urban conditions (Thijsse and van Oss 1997), original references: Schmitz T et al. (1997); Abraham et al. (1994); Bayerisches Landesamt für Umweltschutz (1994); Bruckmann et al. (1983); Ellermann et al. (1995); Thijsse and van Oss (1997)

The choice of the measurement site 5 km downwind of the city centre turned out as a reasonable compromise between the requirements of sufficient mixing of the individual sources of the city and of sufficiently high concentration fluctuations needed for correlations. A good agreement between emission ratios derived from aircraft and from receptor site measurements shows that the emitted pollutants were sufficiently mixed at the receptor site to represent the emissions of the whole city. Thus, it has been shown that this experimental condition is fulfilled, which is necessary for the comparison of measured concentration ratios from long-term measurements with those from the emission model (Mannschreck et al., this issue).

The good agreement of our  $HC_i/HC_{sum}$  emission ratios with the average hydrocarbon composition for German city conditions (Mannschreck et al. 2002b) suggests that the Augsburg emission pattern can be considered as typical for German cities.

### **3.3.3.6 Comparison of two different HCHO Measurement Techniques: TDLAS and a commercial Hantzsch Monitor – Results from Long-term Measurements in a City Plume during the EVA Experiment.**

D. Klemp, K. Mannschreck, B. Mittermaier

#### **Introduction**

For the evaluation of an emission model two field campaigns have been performed in the Augsburg area in March and in October 1998. As part of an integrated concept (Slemr et al. 2002b) of ground-based and air-borne measurements as well as tracer experiments, the long-term measurements were applied to characterize the composition of the city plume of Augsburg. For this purpose, a mobile laboratory was placed 5 km downwind of Augsburg in Stätzling, equipped with analytical instruments for the measurement of NO, NO<sub>2</sub>, NO<sub>y</sub>, CO, C<sub>2</sub> – C<sub>10</sub>-hydrocarbons, HCHO, O<sub>3</sub> and meteorological parameters. In this study special emphasis is placed on the results of atmospheric HCHO concentrations, measured by two different measurement techniques: Tuneable Diode Laser Absorption Spectroscopy (TDLAS) and a commercial Hantzsch monitor.

#### **Experimental**

Formaldehyde and NO, NO<sub>2</sub> and NO<sub>y</sub> were continuously measured over a period of more than 4 weeks at Stätzling in a distance of about 5 km from city centre in March 1998. Analytical instruments for the measurement of HCHO, NO<sub>x</sub> and NO<sub>y</sub> are part of the equipment, which is installed in the air conditioned mobile laboratory of Forschungszentrum Jülich (Klemp et al. 2002; Mannschreck et al. 2002a). The inlets were mounted on a pneumatic mast 10 m above the surface. For all connections PFA tubing (¼ inch OD) were used. In order to compensate for the different time constants (10%- to 90%-increase) of the analytical instruments (TDLAS: ≈ 10 s, Hantzsch: ≈ 150 s, NO<sub>x</sub>, NO<sub>y</sub>: ≈ 10 s) 10-minutes averages were calculated from the base data set.

*Formaldehyde:* The commercial *Hantzsch monitor* detects HCHO by fluorescence of 3,5-diacetyl-1,4-dihydrolutidin (Dasgupta et al. 1988), which is produced from the reaction of HCHO with 2,4-pentadione and NH<sub>3</sub>. Atmospheric HCHO is transferred quantitatively into the liquid phase using a stripping coil, which was kept at a constant temperature of 15 °C. Zero signals were determined by scrubbing HCHO from ambient air using a Hopcalite<sup>®</sup> filter. The instrument was calibrated by a relative and an absolute procedure. Relative calibrations were performed daily using the internal HCHO permeation device. Absolute calibrations were made once a week using a series of liquid standards (2 \* 10<sup>-8</sup> – 2 \* 10<sup>-7</sup> M). With respect to the 10 minutes intervals an average detection limit of 100 ppt (2-σ) and a precision of 10 % at ambient air levels above 1 ppb were achieved during the EVA campaign.

The *TDLAS technique* is based on the monitoring of the specific absorption from a single rotational-vibrational line in the middle infrared spectrum of the molecule of interest. In order to achieve detection limits which allow monitoring atmospheric concentrations of HCHO (detection at  $1605\text{ cm}^{-1}$ ), a White cell (total light path  $\approx 100\text{ m}$ ) at reduced pressure (30 hPa) is used. Due to the reduced pressure the probability of overlap between absorption lines from other atmospheric species is nearly excluded by reducing the pressure broadening of the rotational lines. In combination with 2-f-derivative detection technique (modulation frequency: 12.5 kHz) optical densities of less than  $10^{-5}$  can be measured. The time resolution of this technique is only limited by the exchange time ( $< 10\text{ s}$ ) of the ambient air, which is pumped at the reduced pressure through the White cell. In order to monitor slowly varying background structures which limit the attainable detection limit of the TDLAS, background spectra were monitored every 5 – 10 minutes by adding  $\text{N}_2$  instead of ambient air at the inlet system. Calibrations were performed every 30 minutes by adding a known mass flow of HCHO from a home-built thermostated permeation device to a  $\text{N}_2$  gas stream at the inlet. Ambient air concentrations were calculated from the comparison of the ambient air spectrum with that from the calibration cycle by fitting Voigt-profiles to the respective data sets. The HCHO mass flow of the permeation device was absolutely calibrated by two independent methods: by gravimetry and by colorimetry as described in Harris et al. (1989). For the TDLAS technique a detection limit of 200 ppt ( $2\text{-}\sigma$ , 10-minutes averages) is achieved throughout the EVA campaign and the precision of the TDLAS measurements at more than 2 ppb is calculated to be 10 %.

$\text{NO}_x$  and  $\text{NO}_y$  were measured using two chemiluminescence detectors (ECO Physics, CLD 770AL ppt), a photolytic converter (ECO Physics PLC 760) to convert  $\text{NO}_2$  to NO, and a home-built gold converter to convert  $\text{NO}_y$  (i.e.  $\text{NO}_x = \text{NO} + \text{NO}_2$  and its oxidation products, mainly  $\text{HNO}_3$ ) to NO on a hot gold surface (Fahey et al. 1985), which was directly placed on top of our pneumatic mast in order to avoid  $\text{NO}_y$  losses. NO calibrations were performed daily by adding a known flow of calibration gas (10 ppm NO in  $\text{N}_2$ ) into the  $\text{NO}_x$ -free air stream. The conversion efficiencies of the PLC and the Au-converter for  $\text{NO}_2$  were also determined every night. The conversion efficiency of the Au-converter for  $\text{HNO}_3$  was checked weekly using a home-built permeation source. For NO a precision of 8 % and a detection limit of 20 ppt ( $2\text{-}\sigma$ ) were achieved for an integration time of 10 minutes. The corresponding data for  $\text{NO}_2$  and  $\text{NO}_y$  are 9 % and 30 ppt, and 8 % and 200 ppt, respectively.

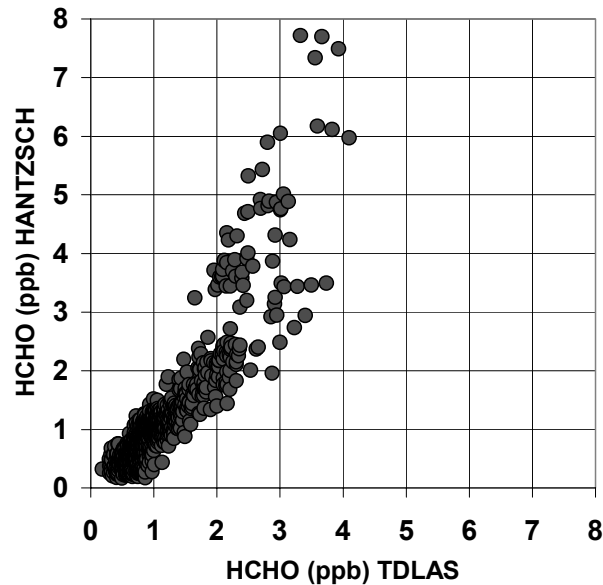
## Results

### Comparison of concurrently measured HCHO concentrations

In Fig. 3.23 more than 1000 concurrently measured 10-min averages are plotted. Only data from the city sector are considered. For most pairs of measurements (i. e.  $\text{HCHO} < 2\text{ ppb}$ ) both detection techniques yield comparable mixing ratios.



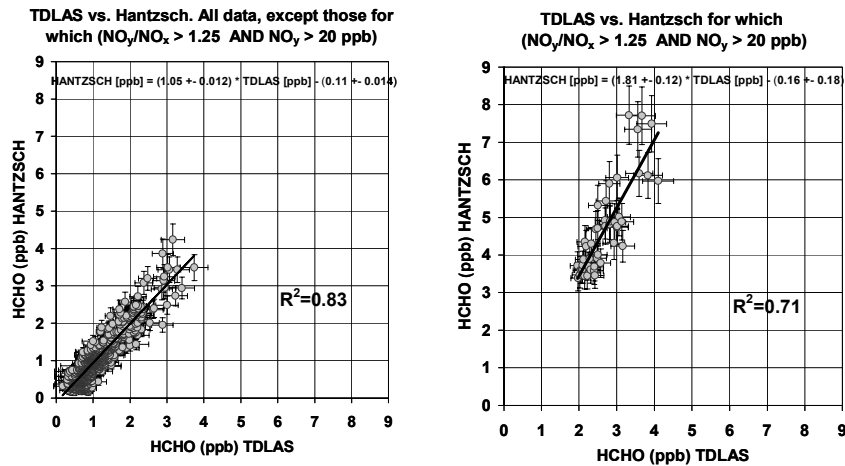
For higher mixing ratios, however, some Hantzsch measurements exceed those of TDLAS by up to a factor of two.



**Fig. 3.23.** Result of concurrently measured HCHO concentrations (Hantzsch monitor and TDLAS, 10 minutes averages) during the EVA campaign (2. 3. – 31. 3. 1998) downwind of Augsburg.

As shown in Fig. 3.24, both subsets of data can be successfully separated by using the  $\text{NO}_x$  concentrations and the respective  $\text{NO}_y/\text{NO}_x$ -ratios as filter criteria. The  $\text{NO}_y/\text{NO}_x$ -ratio is used as a “photochemical clock” in order to calculate the effect of photochemistry on the measured air masses which are transported from Augsburg to the receptor site. Changes in the  $\text{NO}_y/\text{NO}_x$ -ratio of an air mass are mainly caused via OH attack of  $\text{NO}_2$  to produce  $\text{HNO}_3$  (which is the most abundant of the  $\text{NO}_y$  species and which is not emitted directly). That means, the  $\text{NO}_y/\text{NO}_x$ -ratio of an air mass is a measure for its photochemical exposure and for freshly polluted air masses the respective  $\text{NO}_y/\text{NO}_x$ -ratio is always<sup>5</sup> close to 1.

<sup>5</sup> The  $\text{NO}_y/\text{NO}_x$ -ratios in a city plume can be understood as the result of mixing of aged air masses of background air (containing high  $\text{NO}_y/\text{NO}_x$ -ratios but low concentration levels) with fresh  $\text{NO}_x$  emissions. Nevertheless, due to the much stronger  $\text{NO}_x$  increase caused by the impact from the city the resulting  $\text{NO}_y/\text{NO}_x$ -ratios concentration levels yield values of only slightly higher than 1.

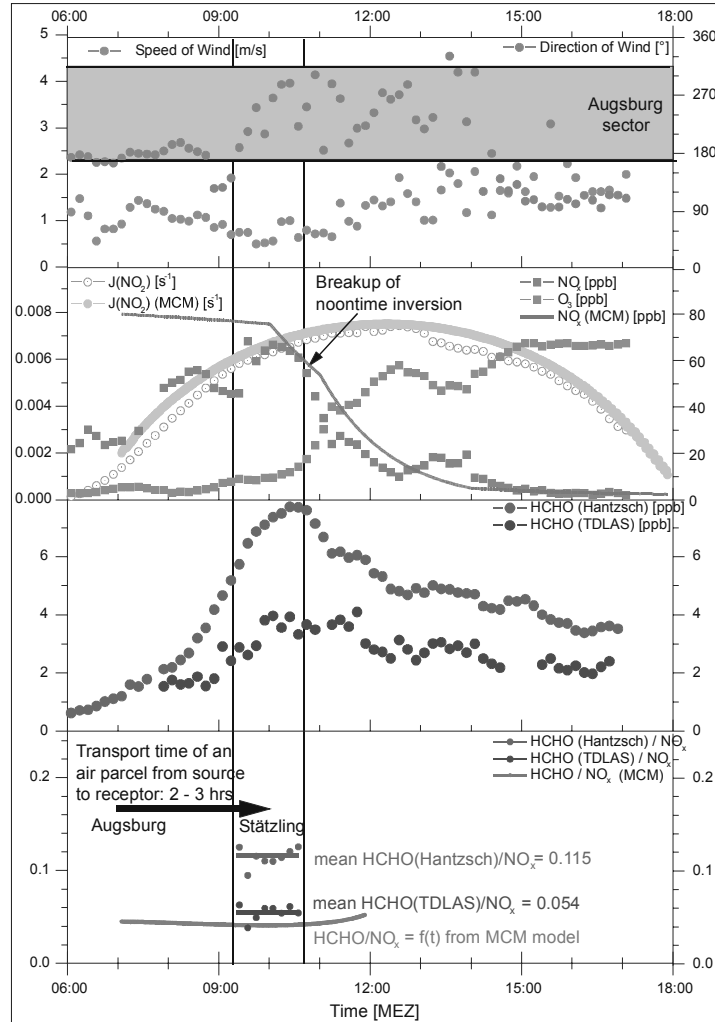


**Fig. 3.24.** Result of correlation analysis (orthonormal regression) between Hantzsch and TDLAS using  $(NO_y/NO_x > 1.25$  and  $NO_y > 20$  ppb) as separation criteria. The error bars denote the respective 2- $\sigma$  errors of the individual 10-minutes averages.

A quite good agreement between TDLAS and Hantzsch in the Augsburg plume is observed in fresh emissions ( $NO_y/NO_x < 1.25$ ) and for low and moderately polluted conditions i.e.  $NO_y < 20$  ppb, ( $NO_y^{\text{Mean(EVA-1)}} = 8.36$  ppb). The orthonormal regression analysis yields a slope of  $HCHO^{\text{HANTZSCH}}/HCHO^{\text{TDLAS}} = 1.05$  ( $R^2 = 0.83$ ). During heavily polluted events ( $NO_y > 20$  ppb) with photochemically active conditions ( $NO_y/NO_x > 1.25$ ) the slope is  $HCHO^{\text{HANTZSCH}}/HCHO^{\text{TDLAS}} = 1.81$  ( $R^2 = 0.71$ ).

If photochemically active conditions connected with high precursor concentrations are excluded from the long-term data set, the HCHO measurements of Augsburg yield an agreement within 5% between Hantzsch and TDLAS. Moreover, from the good accordance between both methods outside photochemically active conditions and from the stability of calibration signals, calibration errors can be excluded to be the reason for the observed deviations.

In principle, with respect to the observed deviations between both HCHO measurement techniques during photochemically active periods two explanations are possible: a positive interference of the Hantzsch technique caused by unknown species or a negative interference, which reduces the TDLAS absorption signal. The latter explanation seems to be rather unlikely. Any interference by an additional species at the same spectral range would even enhance the measured absorption signal of the TDLAS system and could not explain HCHO mixing ratios, which are up to a factor of two smaller than those measured by Hantzsch. Saturation effects of the TDLAS system, which may decrease the sensitivity of the system, can also be excluded: An excellent linearity ( $R^2 > 0.99$ ) of the TDLAS system is observed between 0 and 15 ppb (Klemp et al. 1994).

**Comparison with the results of a box model study**

**Fig. 3.25.** Box model study (MCM, (Derwent et al. 1998)) for the 31. 3. 1998, Augsburg, EVA-1 campaign. Boundary conditions for the MCM box model run: NMHC/NO<sub>x</sub>: 2.5 ppbC/ppb; HCHO/NO<sub>x</sub>: 0.035 ppb/ppb; HCHO background concentration: 0.8 ppb; Mixing height below the persistent inversion layer: 300 m; K<sub>dep</sub>(NO<sub>2</sub>): 0.2 cm/s; K<sub>dep</sub>(HCHO): 0.4 cm/s; a split of 45 individual NMHC was considered.

For a period of summer smog which occurs in the last days of the EVA-1 campaign with substantial deviations between both techniques, a box model study was performed using the MCM model (Derwent et al. 1998). This type of model study leads to reasonable results as long as exchange of polluted air masses from

Augsburg with those from free troposphere is hindered by a stable inversion layer during the morning hours. As shown in Fig. 3.25, air masses from Augsburg are advected to Stätzling from the early morning hours up to 14:00 with low wind speeds of around  $(1.0 \pm 0.5)$  m/s (c.f. upper part of Fig. 3.25). The day is characterized by clear-sky conditions. The break-up of the inversion layer took place at around 10:45, c.f. crossing of the plotted  $O_3$  and  $NO_x$ -lines. Modelled dilution was adjusted in a way that modelled  $NO_x$ -values (start: 80 ppb at 7:00) follow the temporal behaviour of measured values (c.f. second part of Fig. 3.25). HCHO concentrations measured by the Hantzsch system and by TDLAS both show highest levels at around 10:00, like they are also observed for  $NO_x$ , but Hantzsch levels were up to twice as high as the ones measured by TDLAS (c.f. third part of Fig. 3.25). Modelled HCHO/ $NO_x$ -ratios were compared with HCHO(TDLAS)/ $NO_x$ -ratios and HCHO(Hantzsch)/ $NO_x$ -ratios only between 9:15 (minimal transport time, calculated from wind speed and distance from the city) and 10:45 (break-up of the inversion layer). In case of the Hantzsch measurements modelled and measured ratios deviate by more than a factor of two, whereas the respective ratios from TDLAS measurements were close together with the modelled ratios. From the scatter of the individual datapoints it is apparent that the differences between measured ratios are significant.

#### **Mean HCHO/ $NO_x$ -source ratios**

For the calculation of mean HCHO/ $NO_x$ -source ratios from the whole data set only data with wind speeds  $\geq 3$  m/s are used. This approach guarantees for transport times of less than 30 min from the city to the receptor place and it also ensures for neglectable photochemical removal during transport.

Fig. 3.26 shows mean formaldehyde concentrations (based upon 10-minutes averages, measured by a TDLAS system) as a function of  $NO_x$  concentrations. 10-minutes averages of HCHO were grouped by different classes of  $NO_x$  ( $\Delta NO_x = 2$ ppb) and mean formaldehyde concentrations, 25- and 75-percentiles were calculated for each individual  $NO_x$ -class.

Fig. 3.26 suggest two conclusions: i) The regression of HCHO with  $NO_x$  yields an HCHO/ $NO_x$  emission ratio of around  $(3.7 \pm 0.5) \cdot 10^{-2}$  ppb/ppb for fresh emissions. ii) The extrapolation of formaldehyde to the seasonal  $NO_x$  background concentration of 1 ppb (Mannschreck 2001) yields a background concentration of HCHO of  $(0.6 \pm 0.1)$  ppb. This result is in good agreement with the background HCHO concentration of  $(0.7 \pm 0.3)$  ppb observed by us in Jülich-Mersch in March 1995 (Schmitz T et al. 1997).

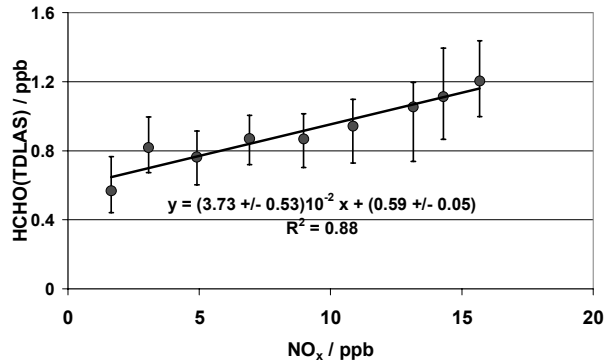


**Fig. 3.26.** Mean formaldehyde concentrations (TDLAS measurements, based upon 10 minutes averages, March campaign) for different NO<sub>x</sub>-classes ( $\Delta\text{NO}_x = 2$  ppb). The error bars indicate the 25- and 75-percentiles of formaldehyde for each NO<sub>x</sub>-class.

The same type of investigation is performed for the HCHO mixing ratios measured by the Hantzsch monitor. Table 3.15 shows that both the HCHO/NO<sub>x</sub> ratios and the HCHO background concentrations are in good agreement for the two independent measurement techniques. Also listed in Table 3.15 is the mean emission ratio of  $\text{HCHO}/\text{NO}_x = 3.3 \cdot 10^{-2}$  ppb/ppb for March 1998 from the emission model provided by IER Stuttgart (Kühlwein et al. 2002a). Within their error limits, experimentally derived HCHO/NO<sub>x</sub>-ratios agree with those from the emission model.

**Table 3.15.** Comparison of experimentally derived HCHO/NO<sub>x</sub> ratios with those from the emission model, provided by IER, Stuttgart (Kühlwein et al. 2002a) for the March campaign. HCHO measurements were clustered by NO<sub>x</sub> intervals and correlation analyses were performed. Two different HCHO measurement methods were used (a commercial Hantzsch system (AL4) and a TDLAS system (TDL)).

	HCHO/NO <sub>x</sub> (ppb/ppb)	HCHO-Background (NO <sub>x</sub> =1 ppb) (ppb)
AL4	$(3.28 \pm 0.48) \cdot 10^{-2}$ $R^2 = 0.82$	$0.49 \pm 0.07$
TDL	$(3.73 \pm 0.53) \cdot 10^{-2}$ $R^2 = 0.88$	$0.61 \pm 0.05$
Emission model	$3.3 \cdot 10^{-2}$	--

### Conclusions

1. An agreement of better than 5 % between Hantzsch and TDLAS is observed for low and moderately polluted conditions.

2. For heavily polluted events under photochemically active conditions the Hantzsch system shows higher values of up to a factor of two. The reasons for this behaviour are still unknown, but there are two arguments which suggest that the Hantzsch HCHO levels are biased by an interference under those conditions:

- The observed  $\text{HCHO}^{\text{Hantzsch}}/\text{NO}_x$ -ratios yield values of around 11%, whereas the  $\text{HCHO}^{\text{TDLAS}}/\text{NO}_x$ -ratios at around 4% (as it is observed as average throughout both EVA-campaigns).
- Additional production of HCHO from chemistry can be excluded from a box model study (initialised by a comprehensive set of measured species) to cause differences of up to 4 ppb during transport from the city to the receptor place 5 km downwind of the city.

Within their error limits, experimentally derived  $\text{HCHO}/\text{NO}_x$ -ratios agree with those derived from the emission model provided by IER.

### **3.3.3.7 Mass balancing by means of vertical and horizontal profiles determined with tethered balloon and airship soundings**

G. Baumbach, U. Vogt, P. Bauerle, K. Glaser

#### **Introduction**

The main target of the joint project EVA (Evaluation of Highly Resolved Emission Inventories) was to determine the mass flow of emissions originating from the whole city containing different sources with the help of ambient air measurements by a combination of ground level, tethered balloon, airship and aircraft measurements.

Here the mass flow calculations windward and leeward of a German city are described, based on results of tethered balloon (vertical distribution) and airship (horizontal distribution) measurements. These experimentally determined results are compared to results of emission modelling.

#### **Measurement strategy**

The emission mass flow of the city of Augsburg should be gained by calculating the difference between the incoming flow of air pollutants windward and the outgoing flow leeward of the city. The principle of the method can be seen in Fig. 3.27. The idea was to set up "virtual windows" windward and leeward of the city in right angles to the prevailing wind direction and to measure the vertical and horizontal distribution of all necessary parameters within these two windows. With tethered balloon (vertical distribution) and airship (horizontal distribution) soundings and additional help of ground level monitoring stations and aircraft flights (horizontal distribution) the windward and leeward concentration fields for  $\text{NO}_x$  and 9 different volatile organic compounds (VOC) and the wind fields could be determined and thus the flows for  $\text{NO}_x$  and VOC could be calculated. Whereas